Supported by Office of Science

Spectroscopic n_e measurements in a recombining divertor region in NSTX using D I high-n series line emission

V. A. Soukhanovskii

Lawrence Livermore National Laboratory, Livermore, CA

R.E. Bell, R. Kaita, A.L. Roquemore

Princeton Plasma Physics Laboratory, Princeton, NJ

Poster TP8.00096

APS-DPP Meeting

Nov. 11-15, 2007

Orlando, FL

College W&M
Columbia U
Comp-X
General Atomics
INEL
Johns Hopkins U
LANL
LLNL
Lodestar
MIT
Nova Photonics
New York U
Old Dominion U
ORNL
PPPL
PSI
Princeton U
SNL
Think Tank, Inc.
UC Davis
UC Irvine
UCLA
UCSD
U Colorado
U Maryland
U Rochester
U Washington
U Wisconsin

Culham Sci Ctr
U St. Andrews
York U
Chubu U
Fukui U
Hiroshima U
Hyogo U
Kyoto U
Kyushu U
Kyushu Tokai U
NIFS
Niigata U
U Tokyo
JAERI
Ioffe Inst
RRC Kurchatov Inst
TRINITI
KBSI
KAIST
ENEA, Frascati
CEA, Cadarache
IPP, Jülich
IPP, Garching
ASCR, Czech Rep
U Quebec

Summary

- Application of Stark broadening measurements of **Balmer** (UV) and **Paschen** near-infrared (NIR) **D I emission lines** for n_e diagnostic of tokamak recombining divertor is presented

  ✓ Several Paschen lines measured for the first time at "low" densities (tokamak divertor - 1 x 10^{19} - 1 x 10^{20} m^{-3})

  ✓ Paschen 4 - 6…14 emission line profiles demonstrate
    - » Substantial Stark broadening (scales as ~$n_e^{2/3}$, l^2 for series)
    - » Low sensitivity to instrumental and Doppler broadening
    - » Good sensitivity to tokamak divertor-relevant densities

  ✓ Comparison with several theoretical models and independent divertor density measurements is commencing

- For the first time, **He II Pfund and Humphrey series lines** have been measured in a recombining NSTX divertor

Divertor emission is recorded spectroscopically in similar high-performance plasmas

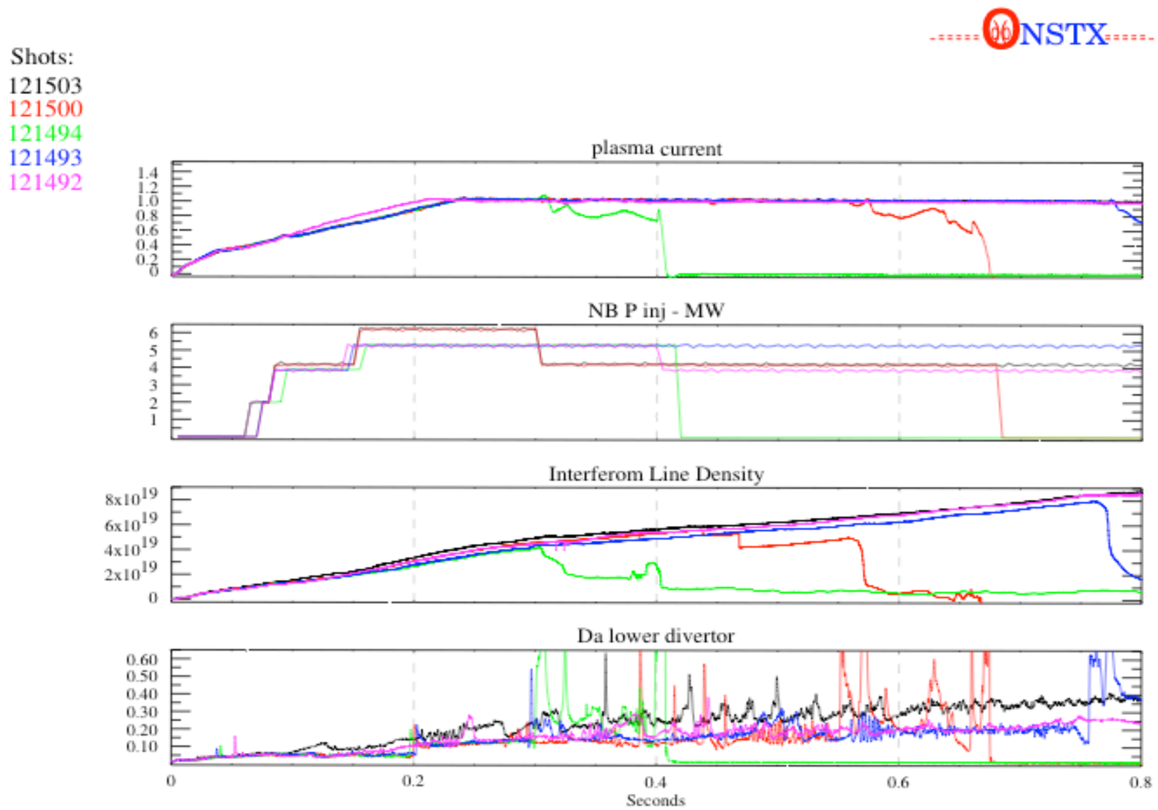

- High performance H-modes
- Inner divertor region is detached (recombining)

Tokamak divertor plasma is well suited for high-*n* series line measurements

- Population kinetics is dominated by 3-body recombination
  - Electron impact excitation much less efficient for high-*n* levels at low T_e
  - 3-body recombination rate is high at high n_e, low T_e
  - Plasma is optically thin for UV-vis-NIR lines

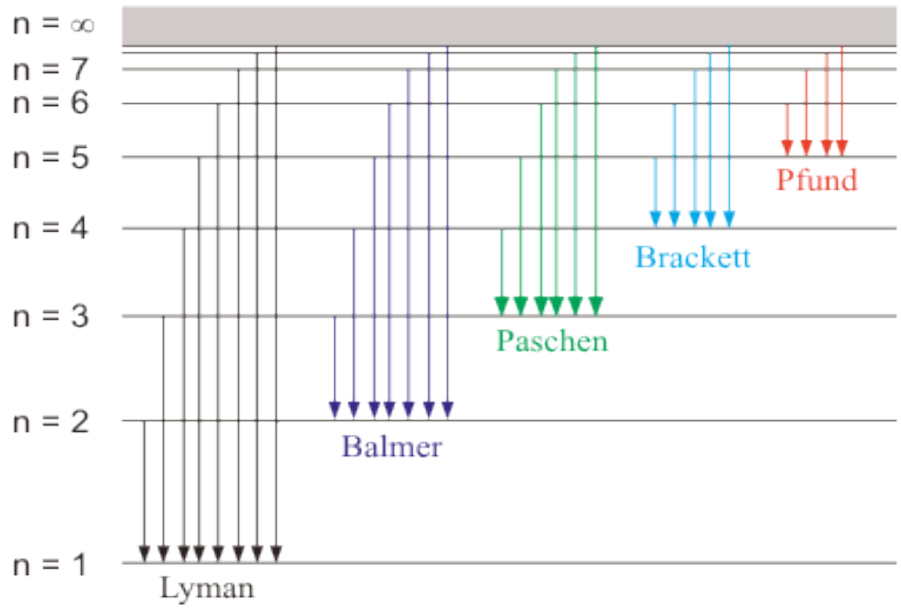

D I:	**VUV**	**UV-vis**	**NIR**	**- NIR -**	**IR -**
He II	**XUV**	**FUV**	**UV**	**UV-vis**	**vis-IR**

- Dominant broadening mechanism: Stark
- Neglected in NSTX: Zeeman spitting, Van der Waals and natural broadening

Reference wavelength of Balmer and Paschen series lines are well known

λ (A)	n_i - n_j	A_{ij}	f_{ij}
3692.605	2-18	3.68E+03	6.10E-04
3698.204	2-17	4.90E+03	7.27E-04
3704.906	2-16	6.65E+03	8.76E-04
3713.027	2-15	9.20E+03	1.07E-03
3722.997	2-14	1.30E+04	1.33E-03
3735.430	2-13	1.89E+04	1.67E-03
3751.217	2-12	2.83E+04	2.15E-03
3771.701	2-11	4.39E+04	2.83E-03
3798.976	2-10	7.11E+04	3.85E-03
3836.472	2-9	1.21E+05	5.43E-03
3890.151	2-8	2.21E+05	8.03E-03
3971.195	2-7	4.38E+05	1.27E-02
4102.892	2-6	9.72E+05	2.21E-02
4341.684	2-5	2.53E+06	4.46E-02
4862.683	2-4	8.41E+06	1.19E-01
6564.610	2-3	4.41E+07	6.40E-01
8440.274	3-18	2.58E+03	9.91E-04
8469.580	3-17	3.44E+03	1.19E-03
8504.819	3-16	4.68E+03	1.44E-03
8547.730	3-15	6.48E+03	1.78E-03
8600.754	3-14	9.20E+03	2.22E-03
8667.398	3-13	1.34E+04	2.84E-03
8752.876	3-12	2.02E+04	3.71E-03
8865.217	3-11	3.15E+04	4.99E-03
9017.385	3-10	5.15E+04	6.98E-03
9231.547	3-9	8.90E+04	1.02E-02
9548.590	3-8	1.65E+05	1.60E-02
10052.128	3-7	3.35E+05	2.77E-02
10941.091	3-6	7.77E+05	5.58E-02
12821.590	3-5	2.20E+06	1.51E-01
18756.13	3-4	8.99E+06	8.42E-01

Lower divertor imaging system enables high spatial resolution spectroscopic measurements

- **Fiber-optic imaging bundle:**
  - Imaging lens - Nikon 85 mm *f* /1.4 lens
  - Mounted on upper window port
  - V-groove design allows focal-plane individual fiber mounting and adjustments during alignment
  - Fiber-optic bundle: eight 1 mm quartz fibers for outer divertor - 1.5 cm spots, 4-5 cm inter-center, twenty four 0.6 mm fibers for inner divertor - 1 cm spots, 2 cm inter-center; total length - 20 m
  - Lines of sight are spatially calibrated with He-Ne laser and computerized measurement arm with *mm-precision*
- **Spectrometer:**
  - Acton Research SpectraPro 500i 0.5 m, *f* / 6.5 Czerny-Turner scheme
  - Three input fibers with *f*-matching optics
  - Three gratings: 600, 1200, 2400 l/mm
  - CCD detector - 1340 x 100 pixel Princeton Instruments Model Spec-10:100B
  - CCD operated in binned mode
  - Typical readout times 15-50 ms / chip
  - Spectrometer and imaging system are photometrically calibrated with URS-600 LabSphere radiation standard *in-situ*

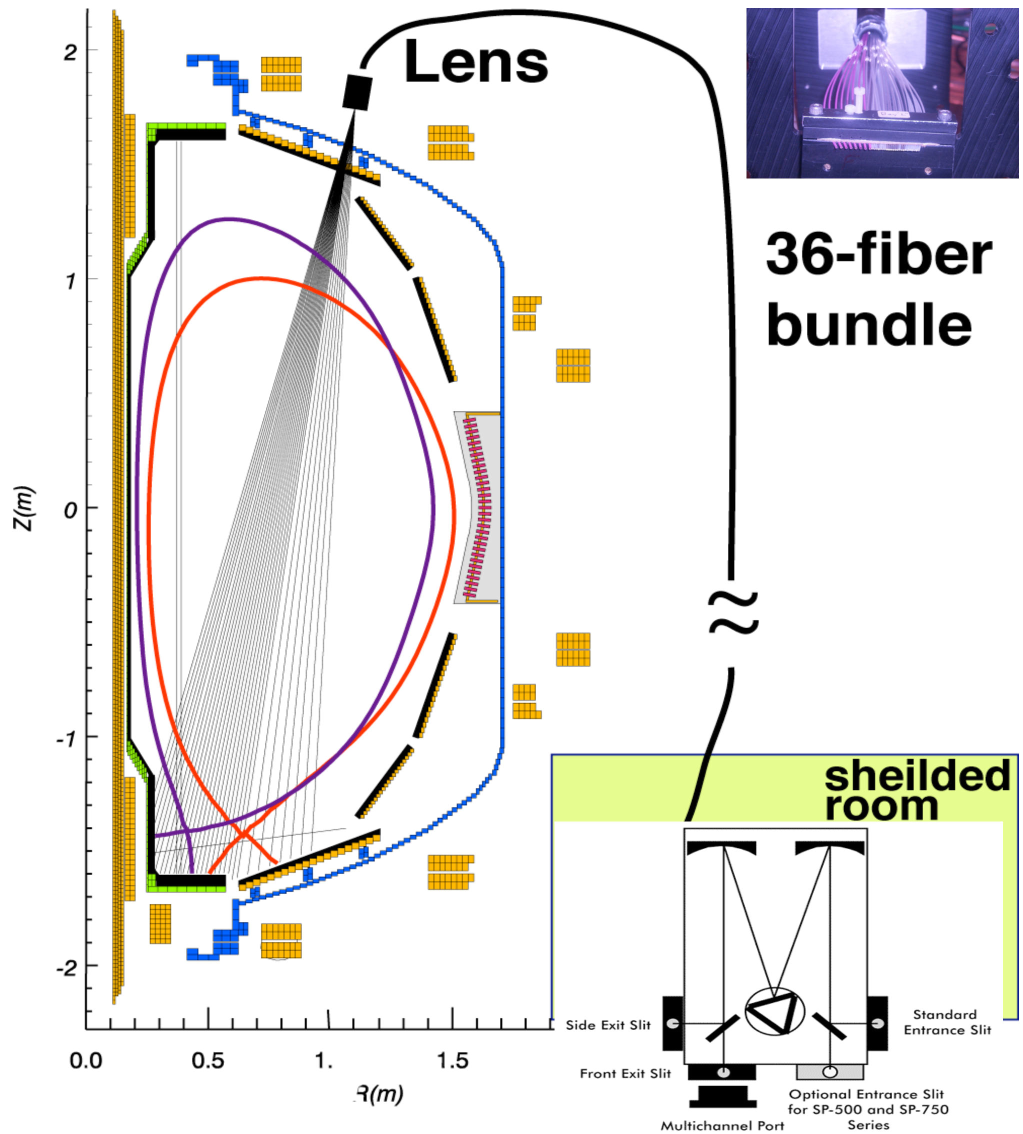

Convolution and measured instr. function are used to obtain pure Stark profiles

- Instrumental function is measured
  - Mercury lamp used
  - For 1200 l/mm grating, instr. function is single Gaussian with FWHM = 1.13 A
  - For 600 l/mm grating, instr. function is not Gaussian. Use Gaussian with FWHM 2.30 A
- Convolution with thermal (Gaussian) FWHM for 2 eV gives FWHM 1.7 A for 1200 l/mm grating, and FWHM = 4 A for 600 l/mm grating

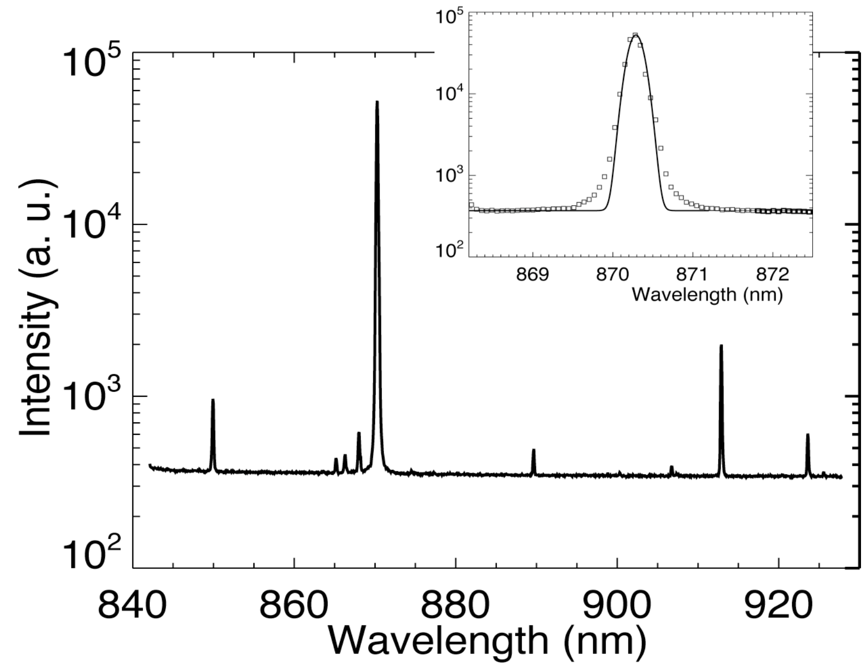

- Spectral analysis procedure:
  - Fit Voigt profile to D lines, Gaussian to impurity lines, with quadratic background
  - $V_{tot} = G_{therm} + G_{instr} + L_{stark} + U_{other}$
  - If $V = G * L$ then $f(V) = f(G) \times f(L)$ and $L = f^{-1}(f(V)/f(G))$, where "*" is integral convolution, f is integral Fourier transform
  - Recover pure Stark profile, fit Lorentzian profile, obtain FWHM and compare to calculations
  - All routines are written in IDL, the MPFIT package is used for line fitting
  - Fourier transforms and convolutions are done numerically

Theory of Stark broadening of deuterium lines has made much progress in last 10-15 years

- Standard theory of Stark broadening
  - Textbook material, e.g. Griem, Sobelman
  - Hydrogen atom: degenerate levels, linear Stark effect
  - Ions: quasi-static microfield distribution (Holtzmark field $F_0 = 2.603\ e\ N_e^{2/3}$)
  - Electrons: impact approximation
  - Well suited for tokamak divertor plasma conditions (T_e < 100 eV, $n_e < 10^{21}$ m^{-3})
  - Useful tabulations: C. R. Vidal *et al*. ApJS 25, 37 (1973), M. Lemke A&A 122, 285 (1997)

- Model Microfield Method (MMM)
  - U. Frisch and A. Brissaud, JQSRT 11, 1753 (1971), C. Stehle and R. Hutcheion A&A Sup. Ser. 140, 93 (1999)
  - Extensive tabulation of line profiles available

- Frequency Fluctuation Model (FFM)
  - B. Talin et. al Phys. Rev. A 51, 1918 (1995); B. Talin et. al. JQSRT 58, 953 (1997); S. Ferri et. al. 14th ICSLS, V. 10, p 115 (1999)
  - Tabulated data fitted to formula $\Delta\lambda = 2.5\ 10^{-13}\ (a\ N_e^{2/3} + b\ N_e)$

Significant volume recombination is observed at outer strike point during detachment

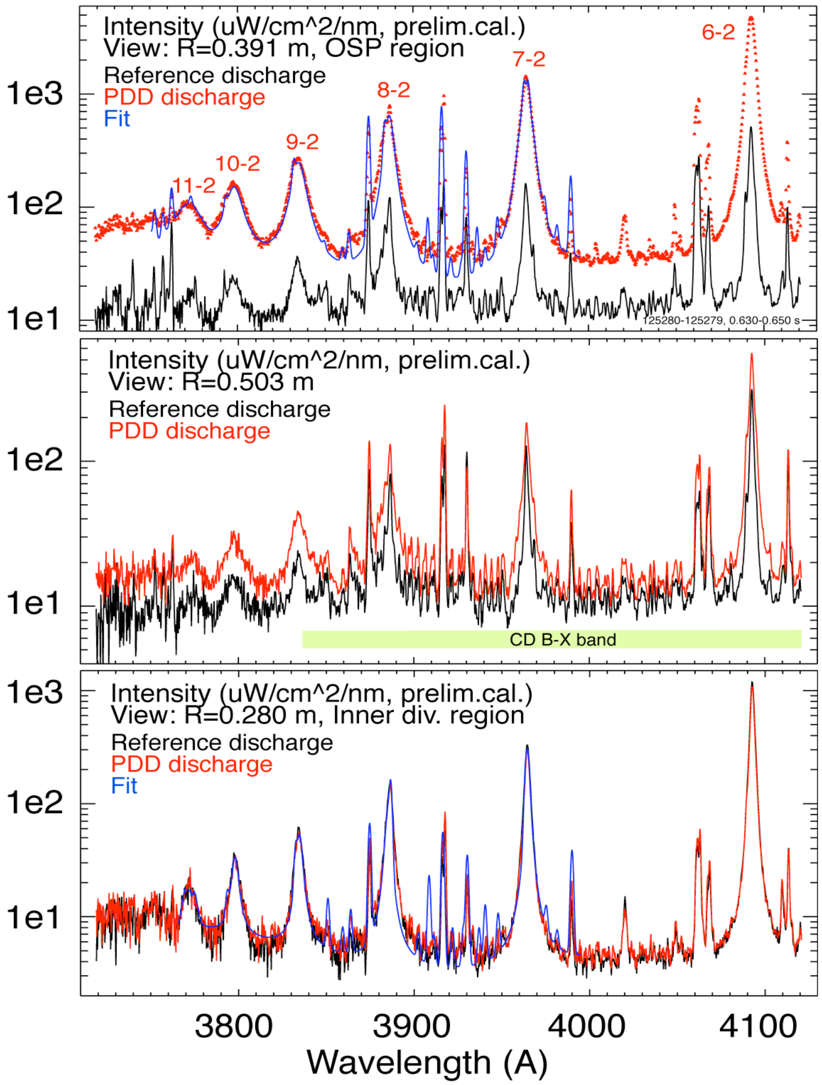

- Balmer series lines 2-6…11
- Sign of strong volume recombination
- Stark broadening yields n_e
- Intensities determined by Saha-Boltzman level population distribution

- n_e ~ 2-3 x 10^{20} m^{-3} in inner divertor (bottom panel)
- n_e ~ 4-6 x 10^{20} m^{-3} at outer strike point (top panel)
- T_e < 1.5 eV
- Interim calibration used
- **Soukhanovskii et. al., Rev. Sci. Instrum. 77, 10F127 (2006)**

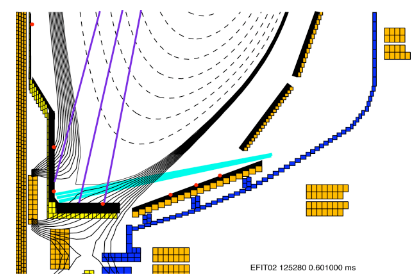

H3 - H15 Balmer lines are observed in detached inner divertor plasma

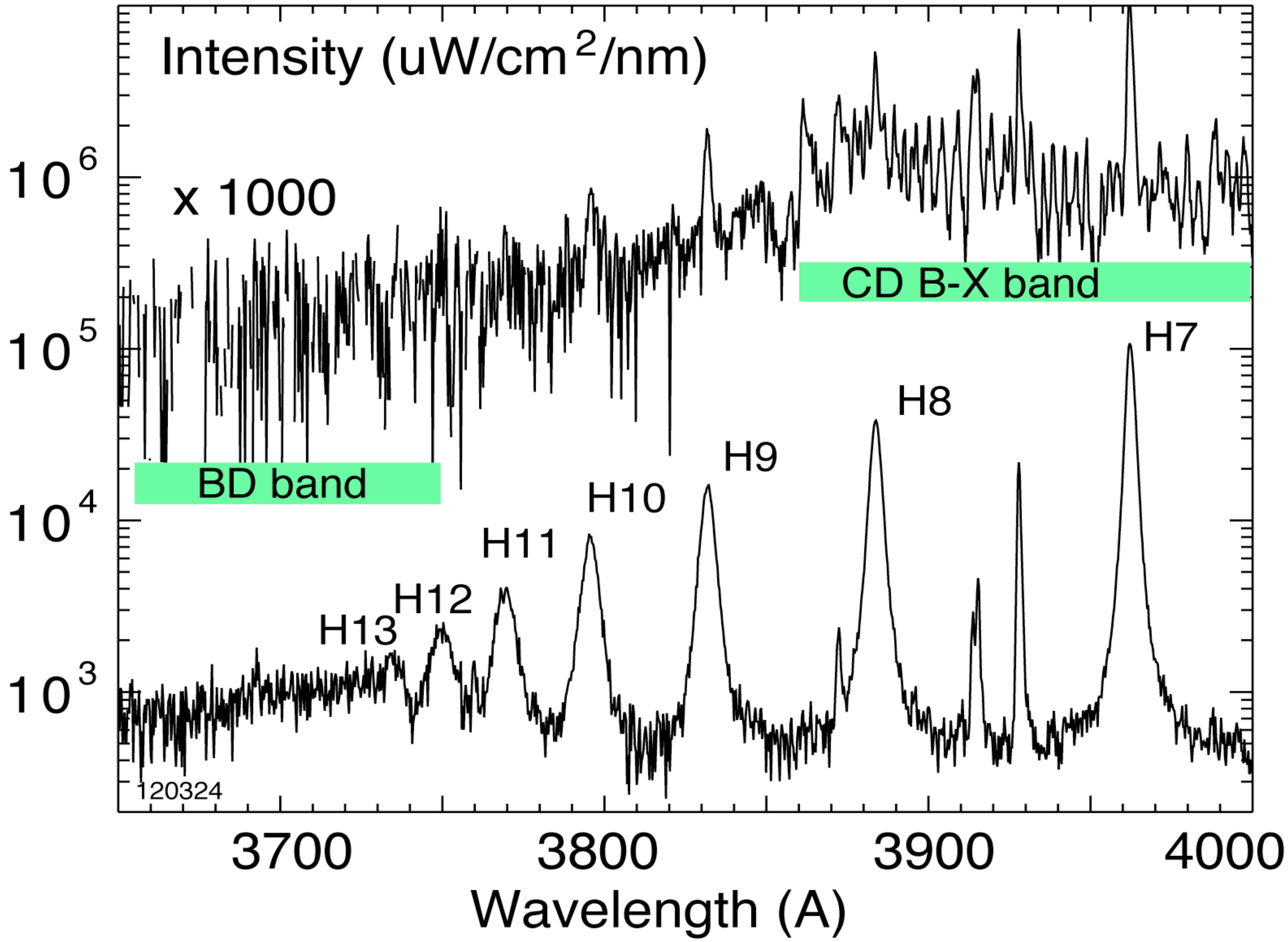

Tabulated Model Microfield Method calculations of Stark profiles used for spectra interpretation

- C. Stehle and R. Hutcheon, Astronomy and Astrophysics Supplement Series 140, 93 (1999)

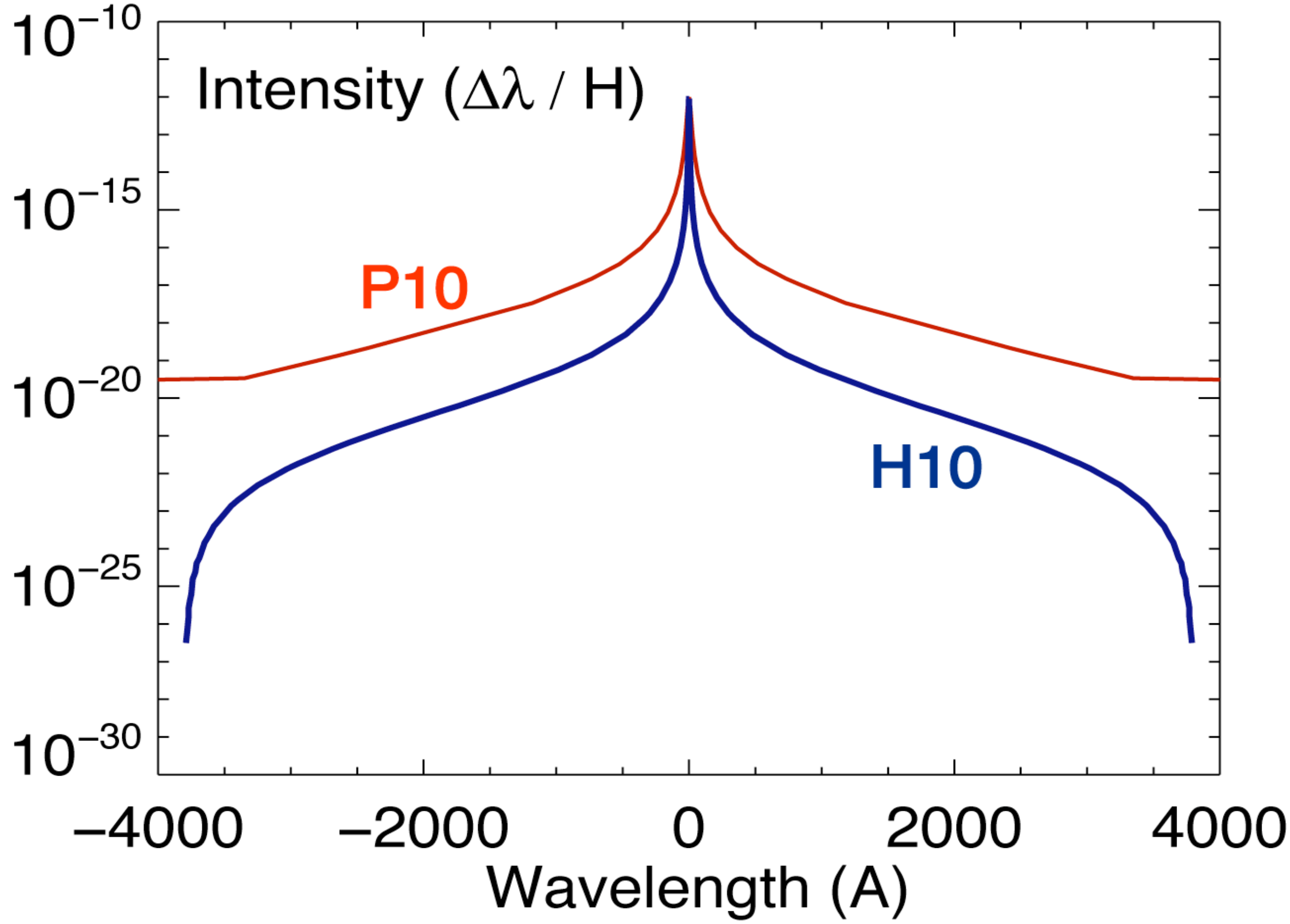

Stark widths of Paschen D I lines sensitive to lower density than Balmer lines

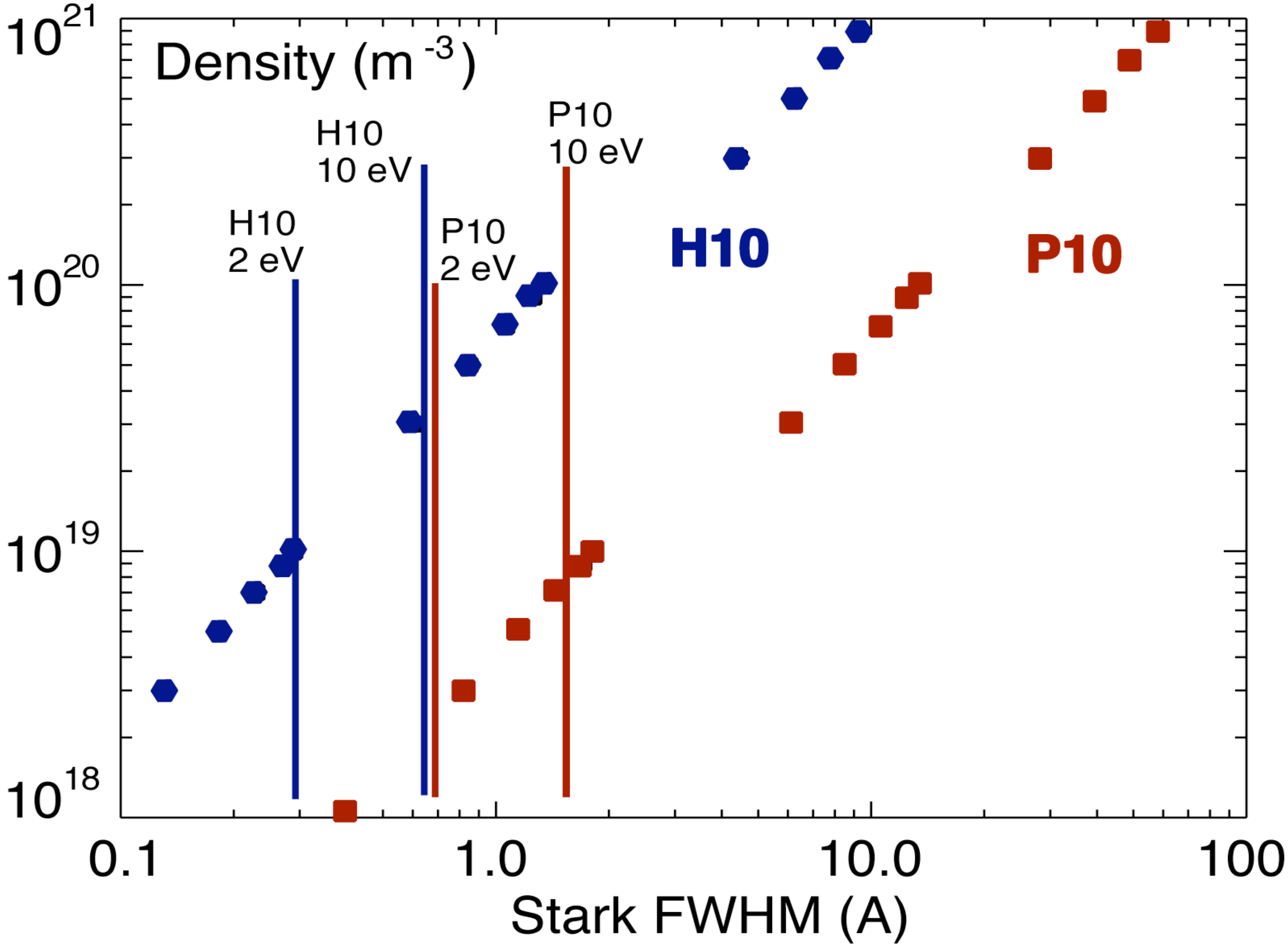

Density comparisons with independent Langmuir probe measurements attempted

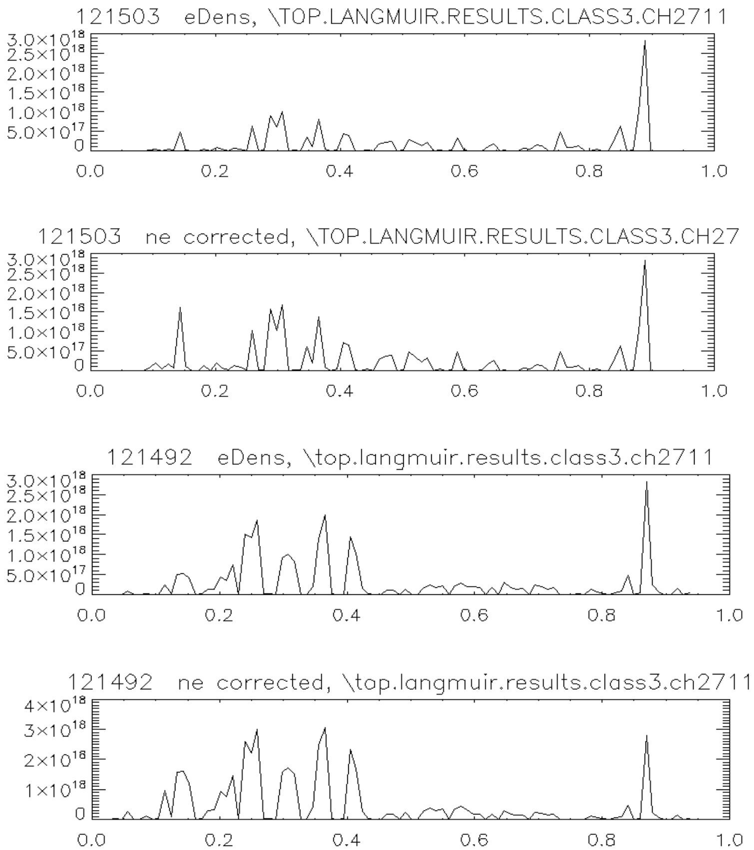

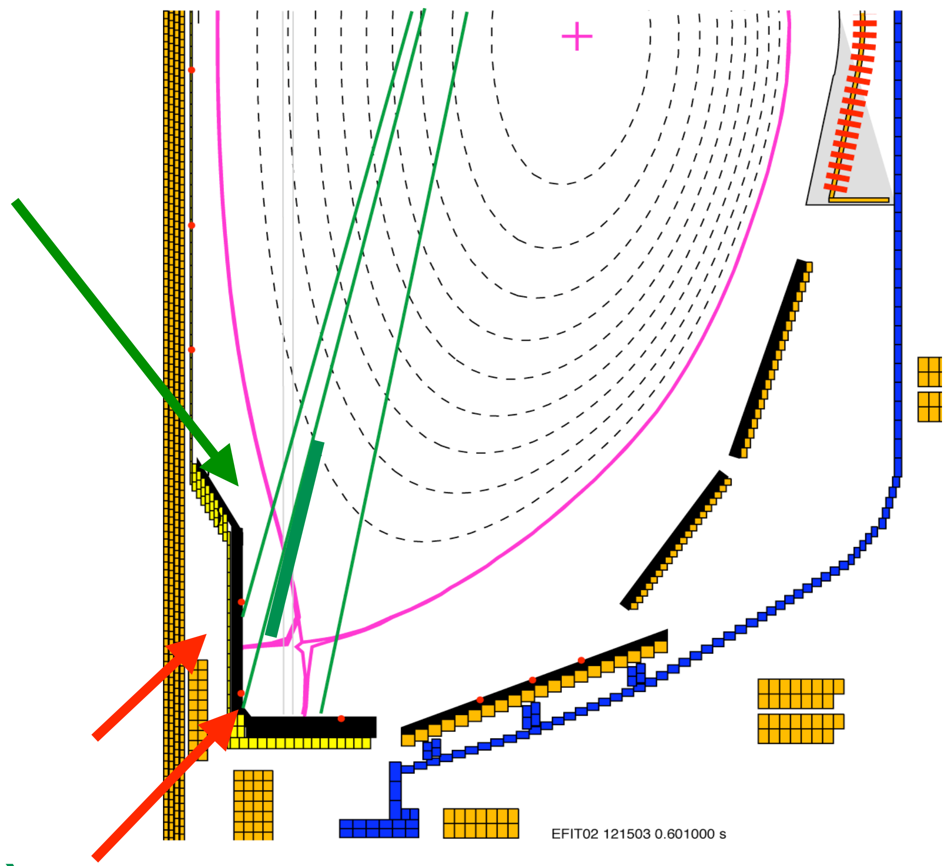

C. Bush (ORNL)

Paschen P6 (P_γ) line is a good candidate for accurate measurements

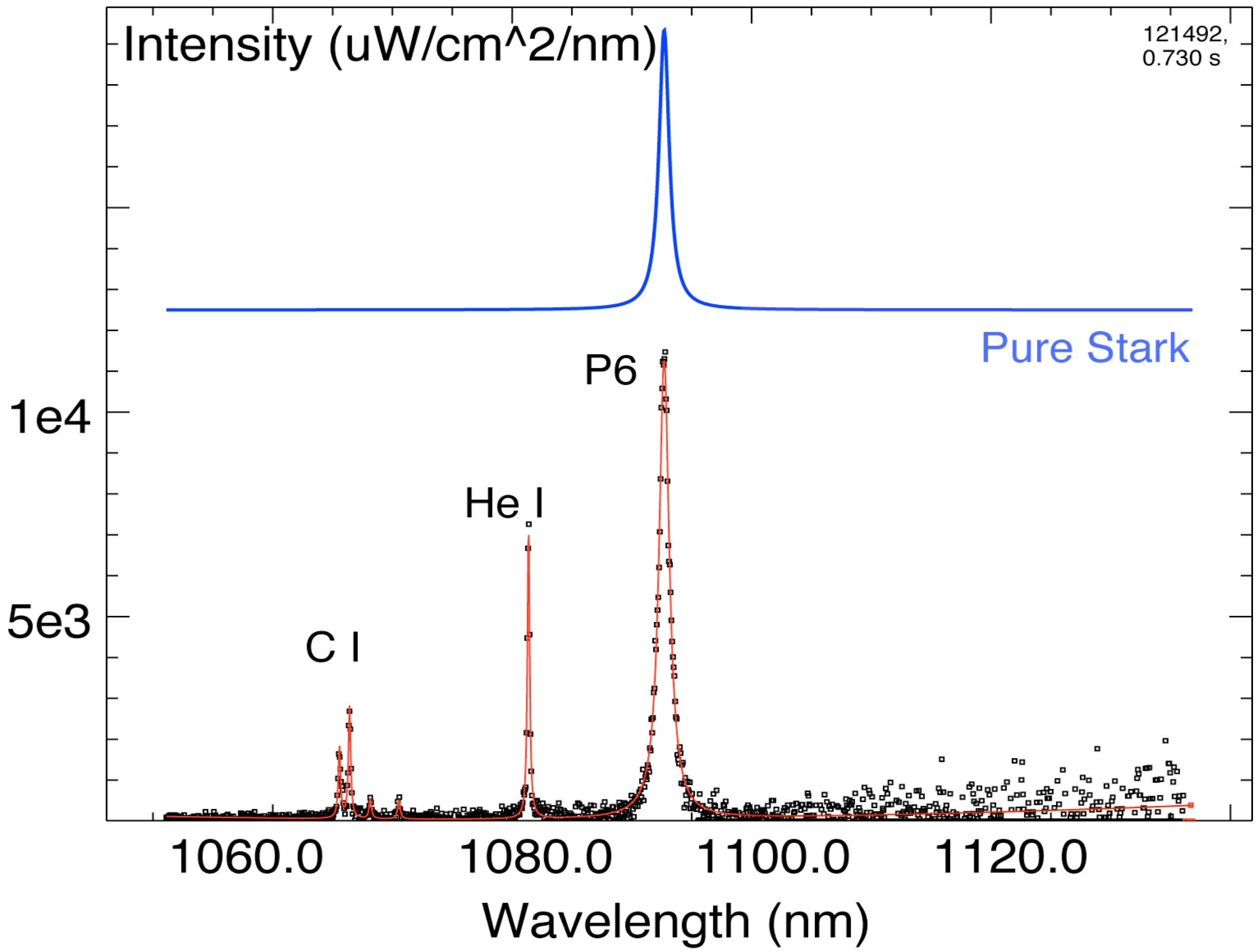

FWHM (nm)	FFM (m^{-3})	MMM (m^{-3})
P6 1.026	-	4.5e20

Paschen P7 (P_δ) line is also a good candidate for accurate measurements

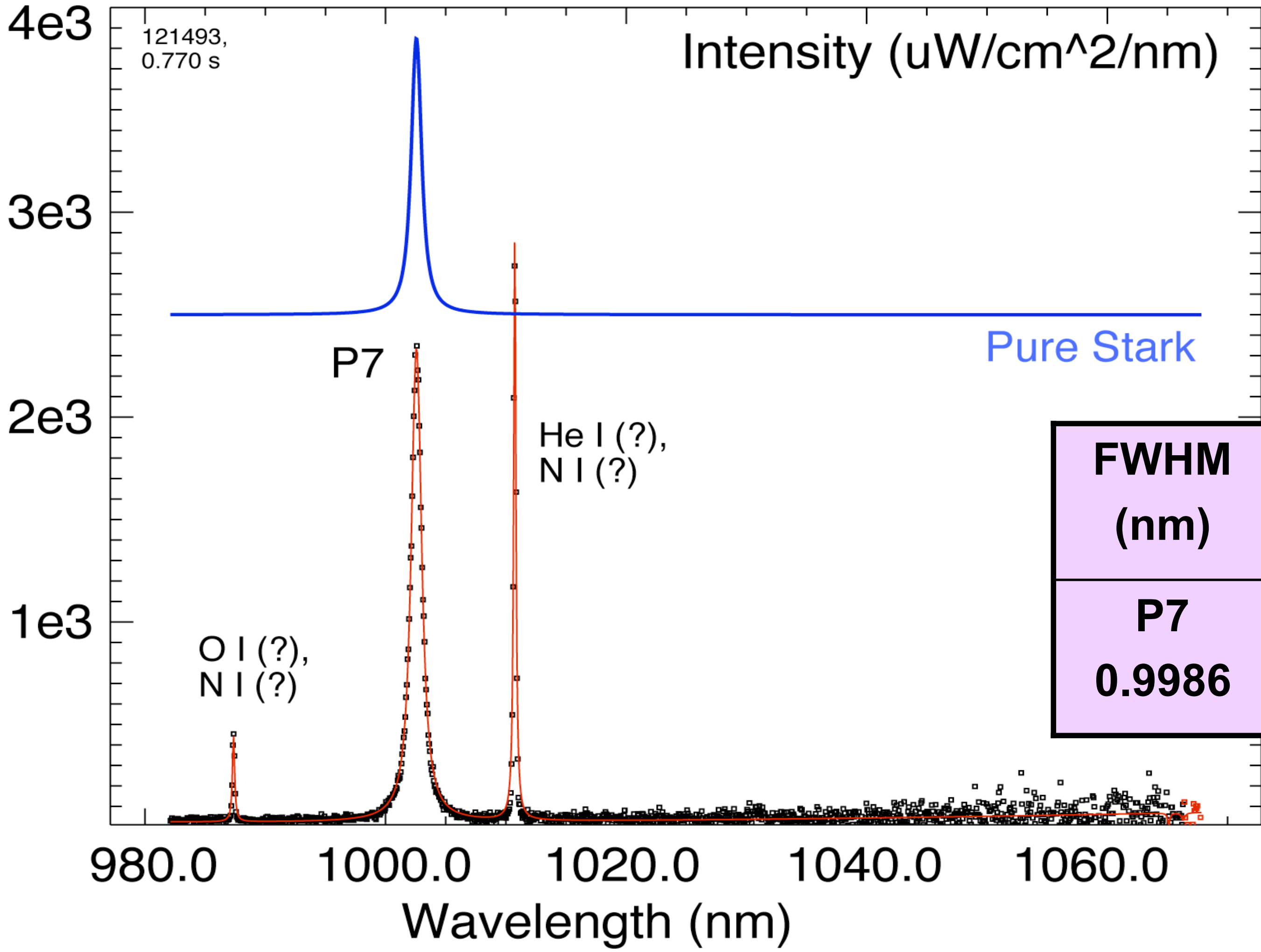

FWHM (nm)	FFM (m^{-3})	MMM (m^{-3})
P7 0.9986	-	2.65e20

Paschen P7 (P_δ), P8 (P_ε) yield consistent divertor densities

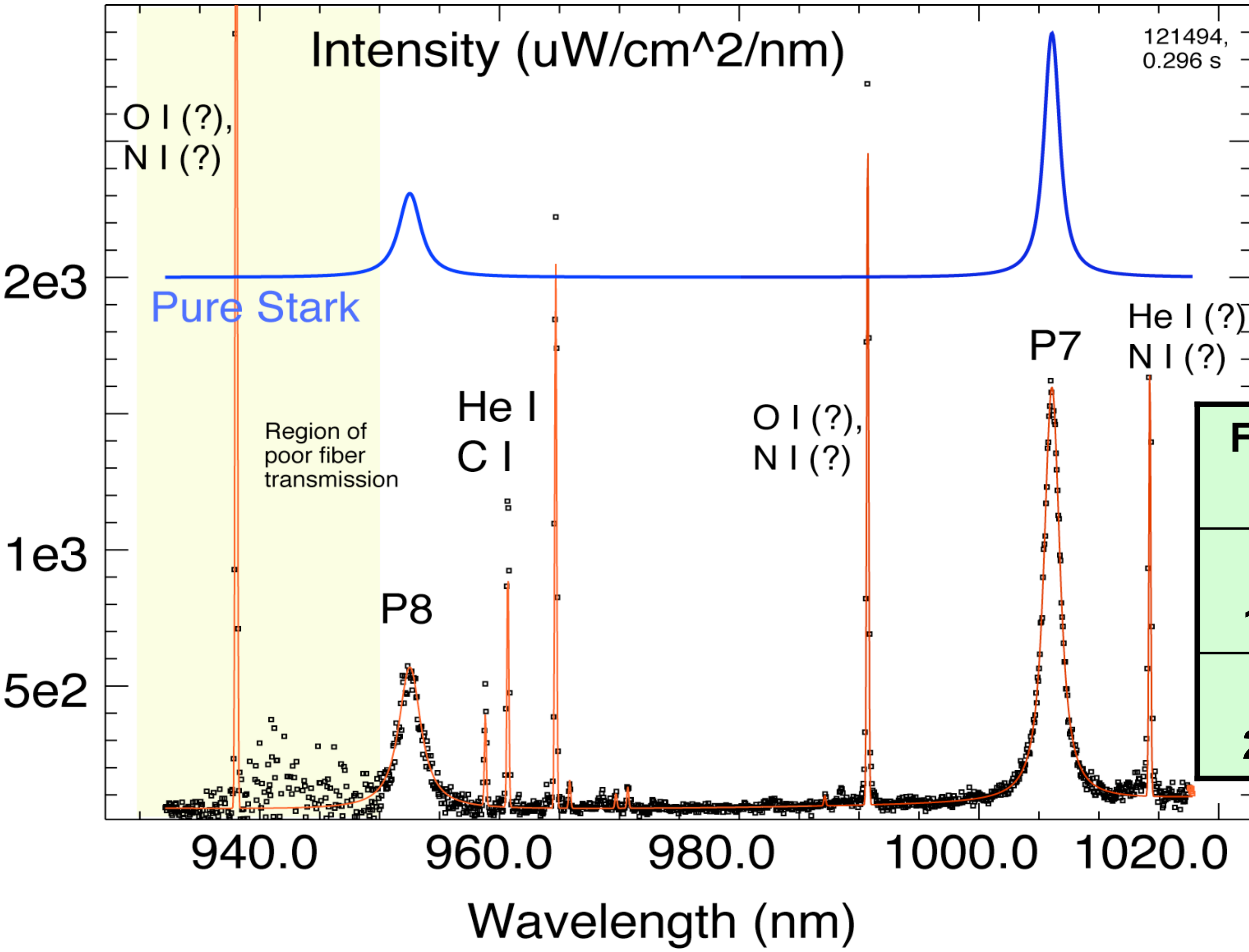

FWHM (nm)	FFM (m^{-3})	MMM (m^{-3})
P7 1.502	-	4.79e20
P8 2.194	4.77e20	4.22e20

- P8 line is adjacent to spectral region affected by NIR fiber transmission

Paschen P8-P11 lines

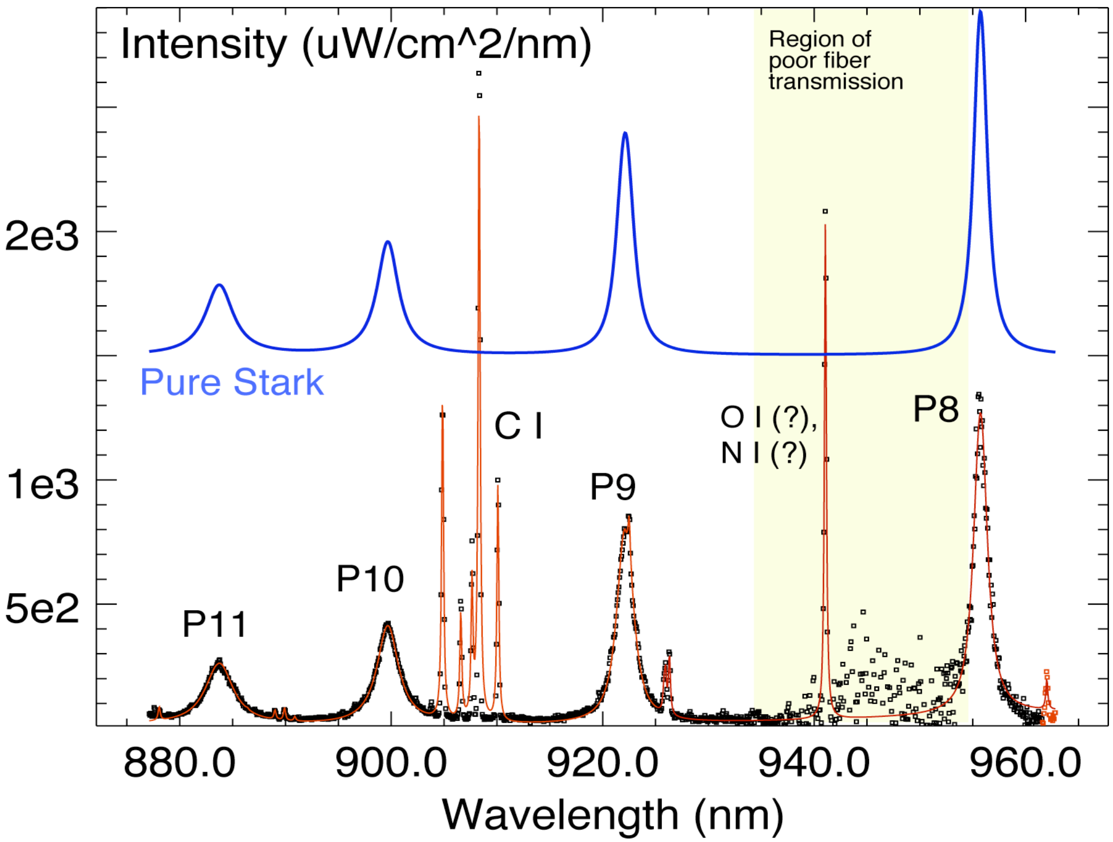

FWHM (nm)	FFM (m^{-3})	MMM (m^{-3})
P8 1.495	2.82e20	2.54e20
P9 1.785	2.27e20	3.04e20
P10 2.476	2.68e20	2.54e20
P11 3.165	2.72e20	3.62e20

- P8 line is adjacent to spectral region affected by NIR fiber transmission
- P9, P10 may be affected by spectral blending

Tokamak recombining divertor measurements enable unique high-*n* Paschen line studies

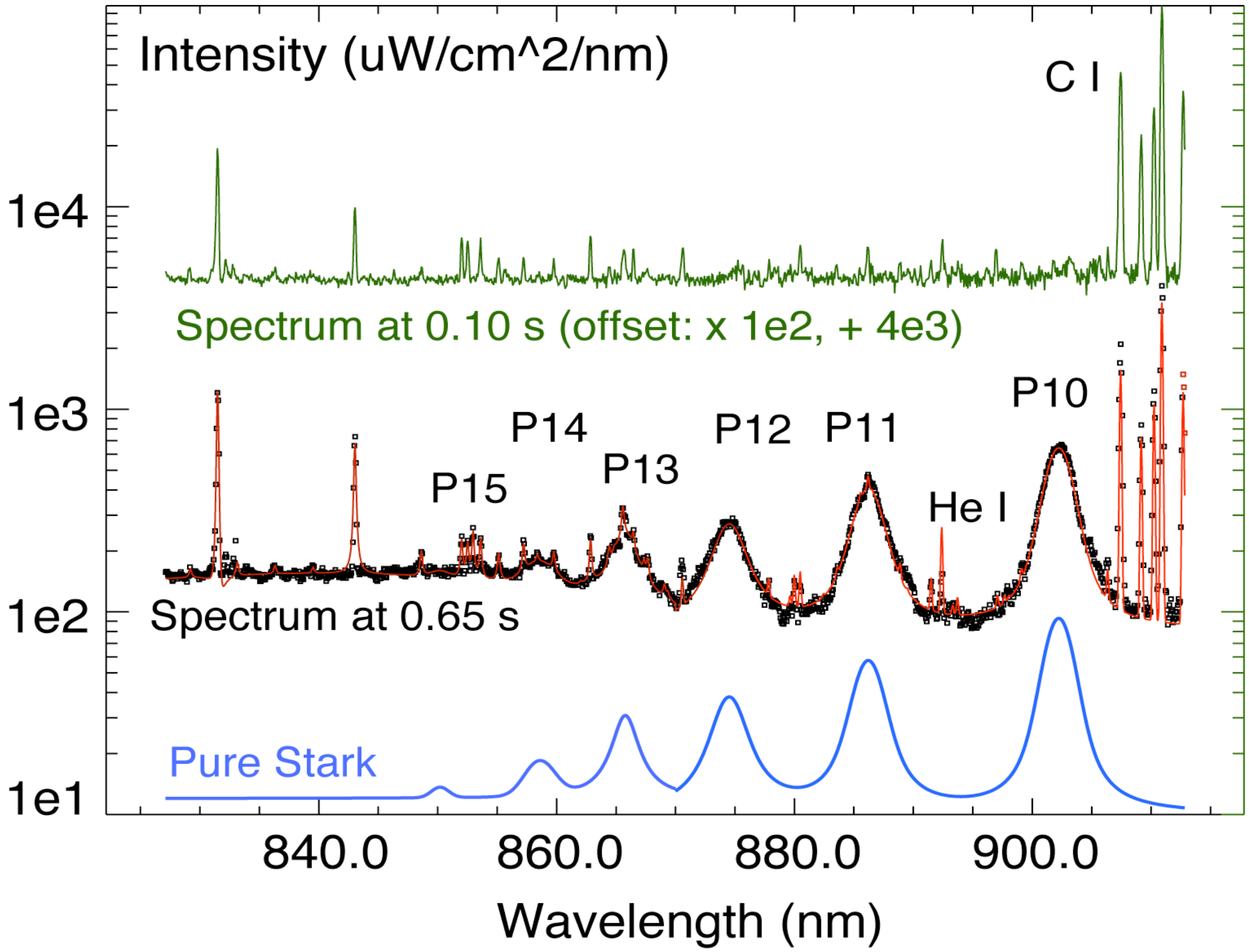

FWHM (nm)	FFM (m^{-3})	MMM (m^{-3})
P10 2.665	2.97e20	2.81e20
P11 2.829	2.32e20	3.02e20
P12 3.198	2.34e20	1.9e20
P13 2.3*	9.87e19	1.13e20

- P11-P15 are severely blended with impurity lines

Paschen P10, P11 lines yield similar densities in inner recombining (detached) divertor region

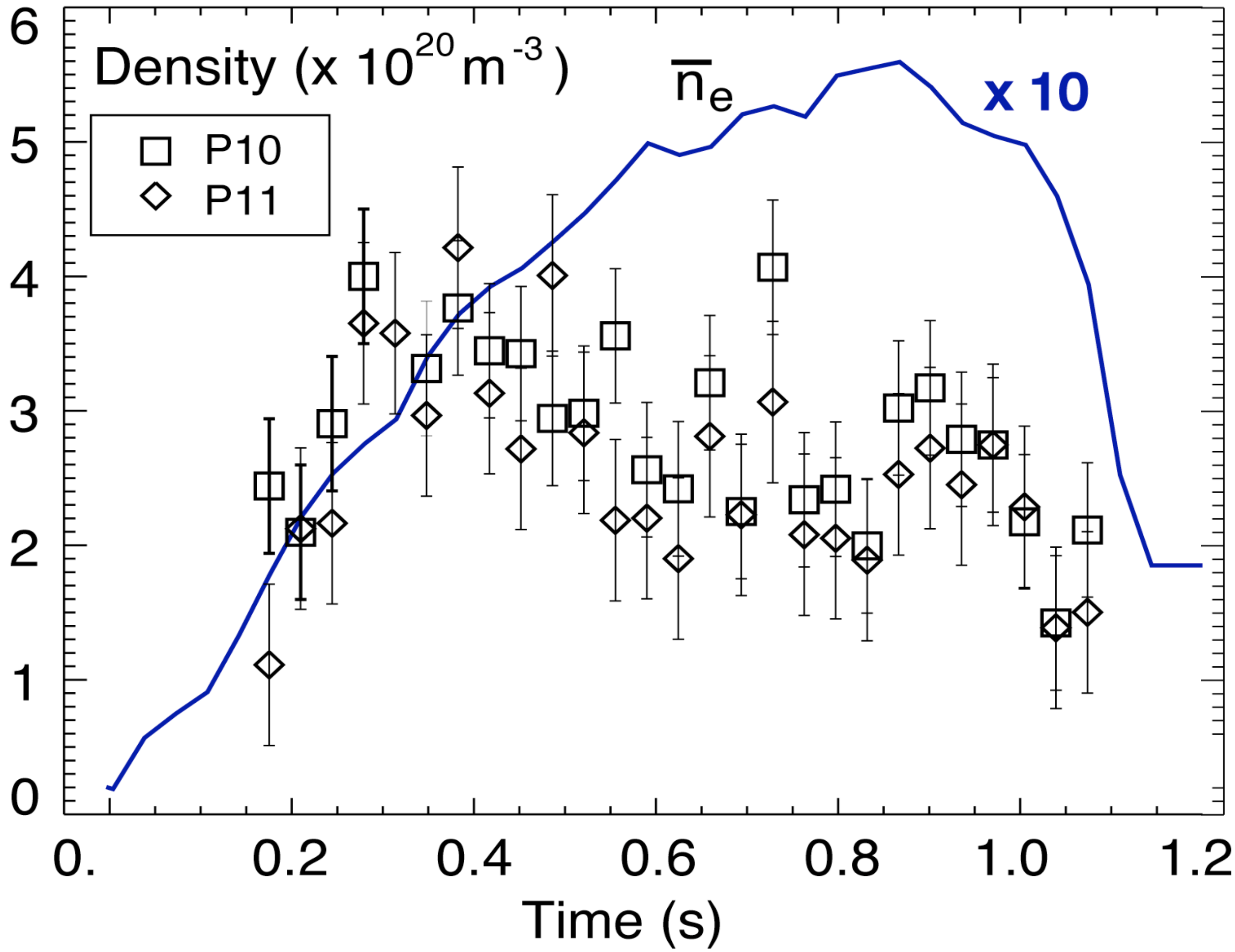

Divertor densities inferred from Balmer and Paschen lines are similar

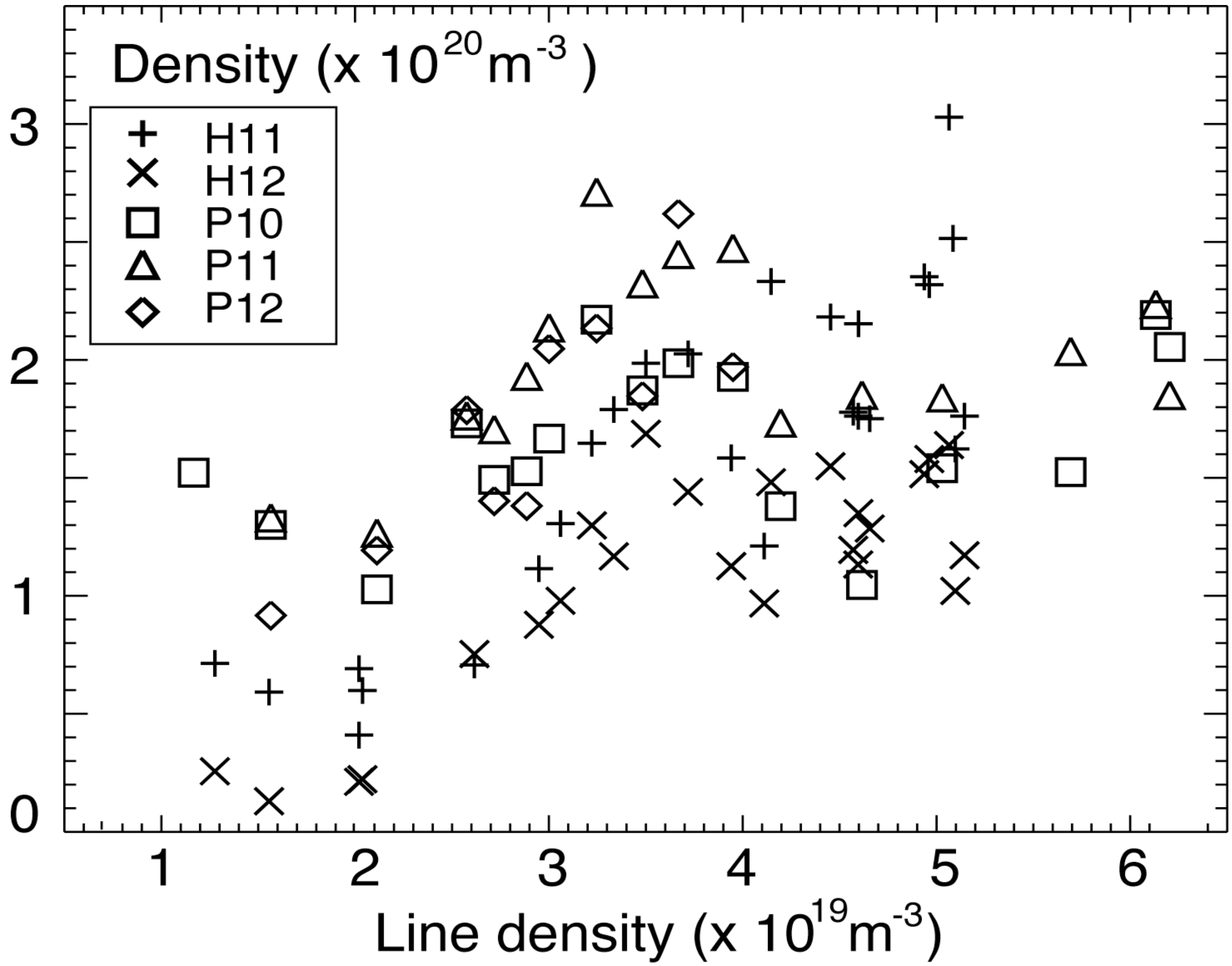

He II Pfund (5-8…19) and Humphreys (6-12…16) series lines have been observed in He plasmas

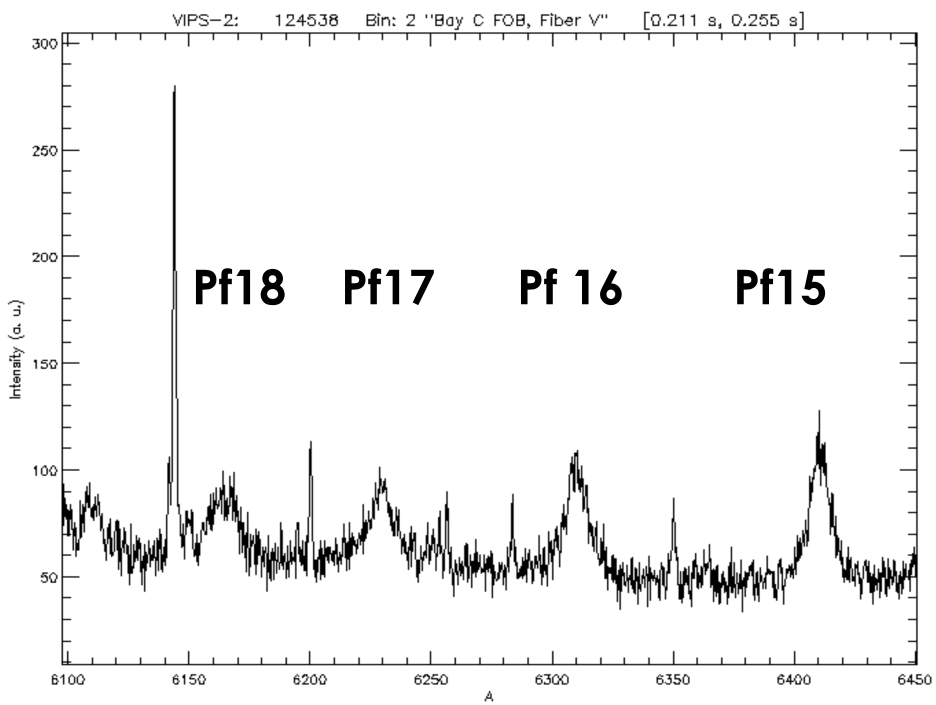

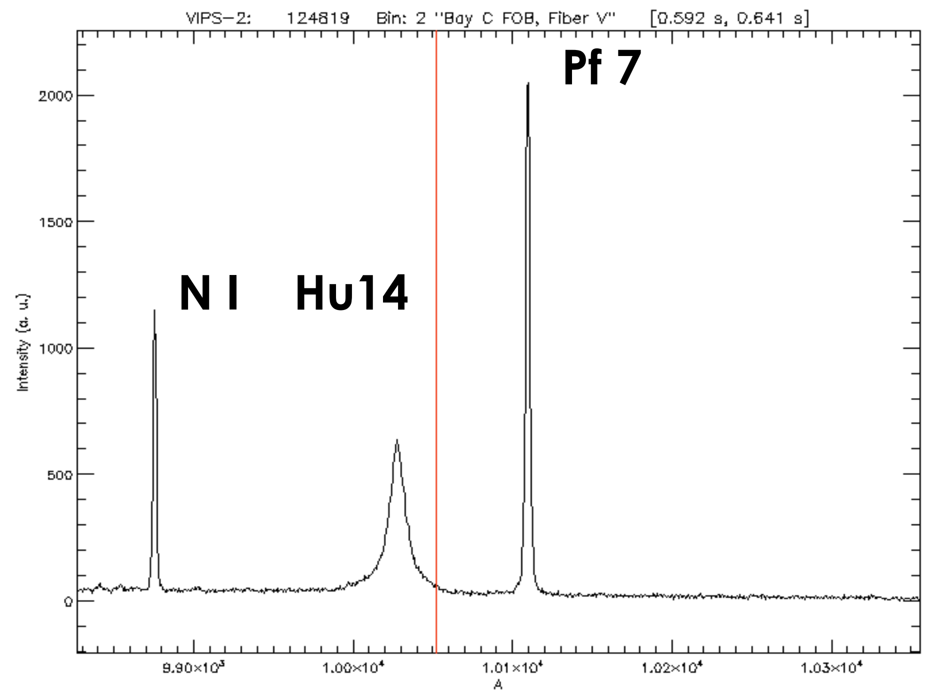

- He II is a hydrogen-like system
- Pfund series lie in visible & NIR range, FWHM ~ 0.5-2 nm
- Humphreys series are in the NIR range, lines are close to D I Paschen series lines
- First observation of high-*n* He II series lines in a tokamak (in laboratory ?)

CRETIN code modeling of Balmer and Paschen spectra is commencing

- Preferred way of analysis - model whole spectrum including bremsstrahlung, line emission, line profiles, self-absorption, ionization and recombination
- Code developed by H. Scott (LLNL)
- Includes non-LTE population kinetics, radiation transport, neutral diffusion, diagnostic simulators
- Line profile code: TOTAL
- Quasi-static approximation for ions, impact approximation for electrons
- Electric dipole momentum reduced matrix elements must be calculated elsewhere
- Good candidate for future analysis

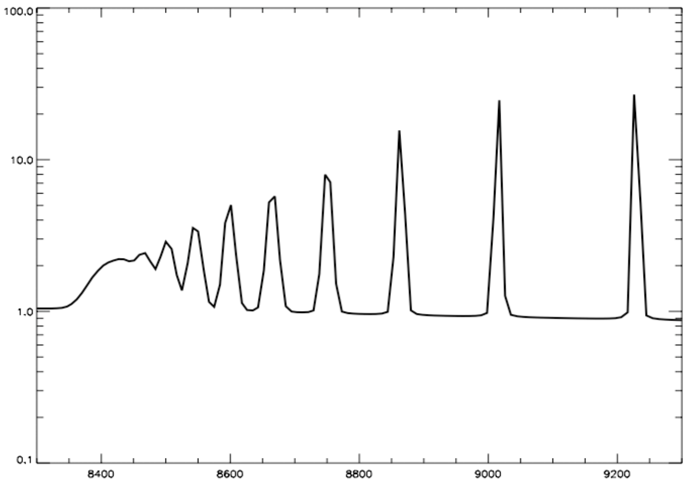

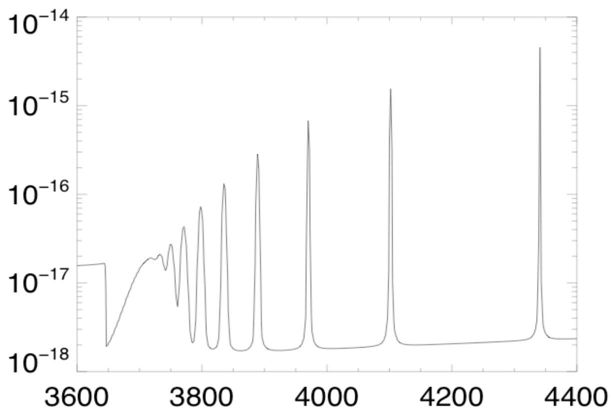

NIR spectroscopy may be a better spectroscopic technique for a burning plasma experiment

- Signal extraction techniques is a big issue for futur burning plasma experiments

- First mirror optical properties (reflectivity, polarization) degrade due to surface erosion and material deposition

- Various materials and mitigation techniques are studied
  - Mo, W, Rh, CU and Stainless Steel
  - mirror materials
  - Single crystal mirrors
  - Polycrystalline mirrors
  - Heated mirrors

$$R = R_0 e^{-\frac{(4\pi d)^2}{\lambda^2}}$$

- Total reflectivity is higher in NIR than in UV-VIS
- Specular reflectance R is a function of wavelength l and mean surface roughness d
- Benett's formula for total reflectivity

Rev. Sci. Instrum. **77**, 10F126 (2006)

D. L. Rudakov et. al.

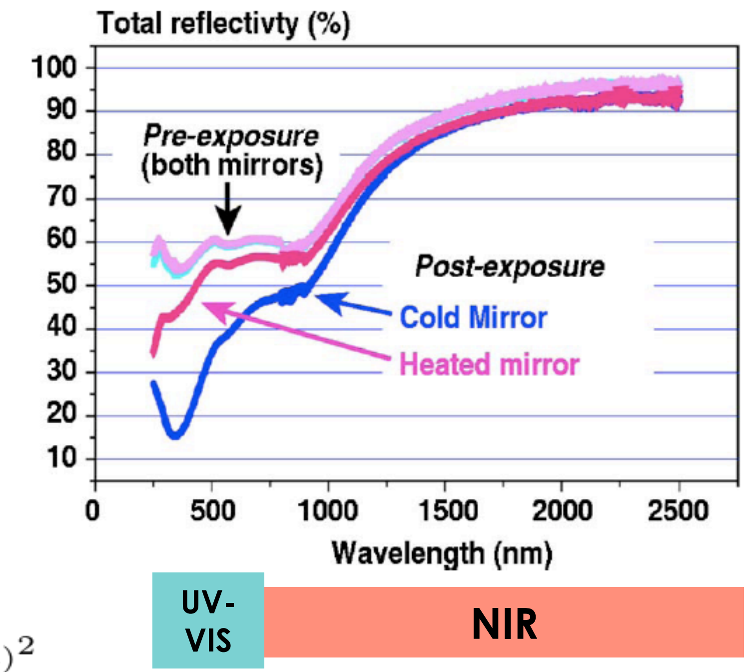

References:
- A. Litnovsky, et. al., to be published, JNM 2007
- M. J. Ruben, et. al. RSI 77, 063501 (2006)
- D. L. Rudakov et. al. RSI 77, 10F126 (2006)
- V. S. Voitsenya et. al. RSI 76, 083502 (2005)

Conclusions and future work

- NIR Paschen lines show good diagnostic potential for divertor-relevant density range
- New imaging spectrometer is needed for multi-channel divertor measurements with existing imaging system on NSTX
- Comparisons with many divertor diagnostics and divertor plasma modeling will be needed for Stark analysis benchmarking
- Rigorous error analysis is in progress
- Analysis based on CRETIN modeling of spectroscopic measurements will be developed

Sign-up